EVS26
Los Angeles, California, May 6 - 9, 2012

Optimal Lightweighting in Battery Electric Vehicles

Johannes Hofer[1], Erik Wilhelm[2], Warren Schenler[1]
[1]*Paul Scherrer Institut, CH-5232 Villigen PSI, Switzerland; E-mail: johannes.hofer@psi.ch*
[2]*Massachusetts Institute of Technology, Cambridge, MA 0213 9-4307, USA*

Abstract

This paper presents an analytic solution to find the optimal amount of lightweighting in a battery electric vehicle (BEV). The additional cost of lightweighting is traded off against the cost savings due to the smaller battery and motor required at constant performance and range. Current technology cost estimates indicate that for a medium sized BEV, optimal glider mass reduction is on the order of 450 kg in 2012 leading to estimated manufacturing cost reductions of 4.9%. Declining powertrain costs are expected to reduce the importance of lightweighting in minimizing BEV cost in the future, and rising electricity costs to increase the gap between the optimal solutions based on minimizing manufacturing versus total costs. The results are strongly dependent on the future development of lightweighting, battery, and electricity costs. The sensitivity of the optimal mass reduction to these critical parameters has been evaluated, and is shown to increase over time.

Keywords: BEV (battery electric vehicle), cost, optimization, light weighting

1 Introduction

Over the last decades rising fuel prices and tighter regulation have stimulated technical developments to improve fuel economy and reduce emissions. Relative to conventional internal combustion engine vehicles (ICEVs), battery electric vehicles (BEVs) constitute a dramatic improvement in vehicle energy efficiency due to the high efficiency of the electric motor. However, their relatively high cost and low range continue to be the great challenges in commercialization. Reducing the energy consumption of electric vehicles is therefore of utmost importance in order to increase range and reduce costs. Besides reduction of vehicle resistances and improvement of powertrain efficiency, a very important option to reduce energy consumption of a BEV is by replacing conventional by lightweight materials. Several studies have evaluated a range of current and emerging technologies in terms of their vehicle energy consumption reduction potential and associated costs [1, 2, 3, 4, 5]. However, technical and economic aspects are usually treated separately, making it difficult to understand how to best implement new technologies. In a recent analysis we have developed a methodology to find the optimum combination of vehicle mass reduction and powertrain efficiency improvement to minimize vehicle lifetime costs [6]. This paper develops an original optimization framework specifically suited to analyze the implementation of lightweighting in BEVs. Lightweighting is beneficial in designing BEVs as it allows a higher range for the same cost, or similarly, a smaller battery and motor at constant range and performance. In the latter case, the driveline costs for smaller and cheaper drivetrain components can be traded off against the higher costs of producing a lighter vehicle glider based on lightweight materials [7, 8]. In this paper we solve for the optimal weight reduction at constant range and performance minimizing either manufacturing or total costs over vehicle lifetime. The approach is fully parameterized, so an optimum is found as a function of vehicle technical characteristics, driving conditions, and technology costs.

The remainder of this paper is organized into five sections. Section 2.1 reviews current lightweighting trends and costs, section 2.2 discusses the influence of vehicle mass on the energy consumption of BEVs, section 2.3 assesses the BEV cost structure today and in the future,

section 2.4 analyses powertrain resizing effects at constant range and performance, and section 2.5 presents the optimization results for the reference sceanrio and their sensitivity with respect to the main cost factors. Section 3 presents the conclusions.

2 Lightweighting of Battery Electric Vehicles

2.1 Lightweighting trends and costs

Reduction of vehicle mass can be achieved by shifting sales from larger and heavier vehicles to smaller and lighter vehicle categories, vehicle redesign, or material substitution [9, 10]. Lightweighting usually refers to reduction of vehicle weight by substituting advanced materials with a higher strength and/or stiffness per weight than traditional materials. This can be realized by replacing, for example, heavier iron or steel parts with high strength steel (HSS), aluminum, magnesium, and/or composite materials such as glass- and carbon-fiber-reinforced polymers. In recent years many low carbon steel parts of vehicle powertrains and body structures have incrementally been replaced by HSS. In fact, HSS content doubled in the last two decades to make up approximately 13% in 2007 [11]. Similarly, aluminum alloys continue to replace low carbon steel, mainly in the engine, transmission, and wheels, but more advanced concepts for all aluminum bodies are implemented. The use of aluminum increased from approximately 5% in 1980 to 9% in 2010 [11]. In addition, there is also an increasing trend towards the use of magnesium, plastics and polymer composites, which account for approximately 0.2% and 8% of the weight of the average US car, respectively [11]. Several major research projects have examined the mass-reduction potential for future vehicles [12, 13, 14, 15]. It is possible to reduce vehicle mass relative to today by approximately 20% with intensive use of HSS, an additional 20% reduction with extensive use of aluminum, magnesium, plastics and polymer composites, and up to 60% with extensive use of carbon fiber composites. Even though some studies indicate that the higher costs of lightweight materials do not increase vehicle costs, actual manufacturing costs are very much dependent on the particular materials used and the associated changes in tooling and assembly. Ultimately, manufacturing costs are expected to increase with the application of advanced materials. Figure 1 shows the estimated additional manufacturer cost per kg reduced as a function of glider mass reduction from a collection of cost analysis [1, 5, 16]. An exchange rate of 0.8 Euro to 1 USD has been used to compare reports prepared in different currencies. All prices are inflation adjusted to 2011 according to the US consumer price index. An exponential cost function has been used to predict for increasing marginal costs for increasing weight reduction

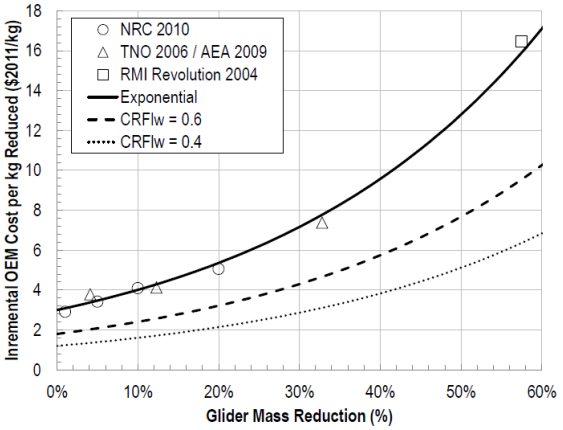

Figure 1: Lightweighting cost estimates [1, 5, 16] and exponential marginal cost function.

$$\mathrm{MC_{lw}} = \mathrm{CRF_{lw}} \cdot \mathrm{a} \cdot \mathrm{e}^{\mathrm{b} \cdot \Delta \mathrm{m_{lw}}} \tag{1}$$

A fit to the data points shown in Figure 1 with an exponential cost function of the form of Eq.(1) yields a = 3 and b = 2.9. Although many individual lightweighting options are mutually exclusive, these studies represent the gross aggregation of many options that lead to the choice of this smoothly continous cost model. To express marginal costs as a function of kg glider mass reduction instead of % reduction, the coefficient b has to be expressed relative to the baseline glider mass. The baseline vehicle configurations described in the following sections form the basis for the application of lightweight materials. It is assumed that the selected glider material composition and lightweighting marginal cost curve is representative for the reference midsize BEV. If a different reference material composition is assumed, the lightweighting cost curve needs to be adjusted accordingly. A cost reduction factor $\mathrm{CRF_{lw}}$ is introduced to describe future cost reductions due to learning effects and mass production. It is used in section 2.5 for scenario and sensitivity analysis. Lightweighting costs $\mathrm{C_{lw}}$ as a function of weight reduction are found by integrating the marginal cost function

$$\mathrm{C_{lw}} = \int \mathrm{MC_{lw}} \cdot \mathrm{d}(\Delta \mathrm{m_{lw}}) \tag{2}$$

$$= \frac{\mathrm{a}}{\mathrm{b}} \cdot \mathrm{CRF_{lw}} \cdot \left(\mathrm{e}^{\mathrm{b} \cdot \Delta \mathrm{m_{lw}}} - 1\right) \tag{3}$$

2.2 Energy consumption and influence of vehicle mass

This section explains the approach used to calculate the energy consumption of the baseline BEV configuration as shown in Table 1, as well

as how to determine its sensitivity to mass reduction. The chracteristics in Table 1 are assumed to be representative for a midsize BEV in 2012. The values for vehicle mass, motor power, battery capacity, and retail price are based on BEVs in the medium passenger car segment (e.g. the Nissan Leaf, Renault Fluence Z.E., etc.) from a review of electric vehicles currently on the market or in development. Estimates for vehicle frontal area A_f, aerodynamic drag c_d, and tyre rolling resistance c_r are based on typical values found for these vehicles and comparison with other sources [20]. In terms of materials, current BEV models are mostly based on previous ICEV model. Exceptions include the BMW i3 (CFRP body, aluminium chassis), the VW e-Up (HSS), or Tesla S (aluminum body). As such it is reasonable to assume that ...

Table 1: Baseline vehicle characteristics for the 2012 medium segment BEV.

Mass (kg)	1500
Power (kW)	87
Battery capacity (kWh)	25
Retail Price ($2011)	43000
A_f (m^2)	2.2
c_d (drag coefficient)	0.28
c_r (rolling resistance coefficient)	0.008
Battery type	Li-Ion
Motor type	PMSM
Transmission	Single-speed

To model the energy consumption of the baseline BEV and to assess its sensitivity to mass, we employ a backward facing vehicle simulation [21, 18] implemented in MATLAB/Simulink in combination with a parametric analysis of energy demand. The backward simulation starts by calculating the tractive power required at the wheel over a predefined driving cycle. In the following we use the New European Driving Cycle (NEDC), the standard test cycle for emission certification of light-duty vehicles in Europe. It consists of four repeated urban sections followed by an extra-urban part. Though there are concerns about the appropriateness of the NEDC in assessing real-world emission levels of ICEVs [19], we assume that it captures the basic kinematic properties of BEV driving and that a scaling factor can be introduced if necessary or the results adjusted to another driving cycle. The model structure is illustrated in Figure 2, including the three main powertrain components of a BEV generating losses, i.e. transmission, motor/inverter, and battery. Based on current BEV designs we consider a single-gear transmission, permanent magnet synchronous electric motor, and a Li-ion battery [17, 22, 23, 24, 25]. To model the efficiency of the motor and inverter we use ORNL measurement data of the 2004 Toyota Prius combined permanent magnet motor/inverter efficiency map [27]. The Prius motor can deliver a peak power output of 50 kW from 1200 to 1540 rpm. In order to match this peak power to the requirement listed in Table 1, we linearly scale the motor torque and assume the efficiency remains unaffected. Using this approach we find an average cycle efficiency of motor/inverter on the NEDC of 79%. In addition, we assume mechanical drivetrain losses of 3% [28], and an average accessory load of 1.5 kW [25, 26]. Note however that accessory loads can be much higher in extreme weather conditions.
Batteries are the most expensive and technically most challenging component of a BEV. Therefore consideration of battery lifetime and cycle efficiency is essential in optimizing the techno-economic performance. Two common forms of models employed [29] are the electrical equivalent circuit [30] and models based on the first principles of electrochemistry [31]. Most studies conclude that efficiency and lifetime depend, among other things, on cell temperature, charge/discharge rate, state of charge, and depth of discharge. It is out of the scope of this analysis to model these effects, instead we use appropriate results from the literature. Similar to [32, 28, 33, 35] we assume an average discharge/charge efficiency of 98% for Li-ion batteries used in BEVs on the NEDC. Targets set by car and battery manufacturers for calendar and deep-cycle life are typically about 10 years and 5000 cycles, respectively. However, it is not yet clear whether current batteries can meet these targets, especially at more severe ambient temperatures [22]. In this analysis we assume a calendar life of ten years for average use at moderate temperature.

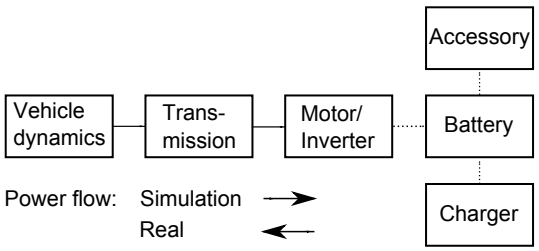

Figure 2: Schematic of the BEV model structure in backward simulation.

In order to estimate the dependence of energy consumption on mass, and hence the influence of weight reduction on energy use, we quickly review the basic equations of motion governing longitudinal vehicle dynamics. On a flat road, the mechanical power at the wheel P_w is given by

$$P_w = P_a + P_r + P_m \tag{4}$$

where P_a is the power necessary to overcome aerodynamic drag, P_r rolling resistance, and P_m the power necessary for acceleration or power available from deceleration. The individual contributions of P_a, P_r, and P_m to the mechanical

power at the wheel P_w acting on the baseline vehicle driving the NEDC are shown in Figure 3.

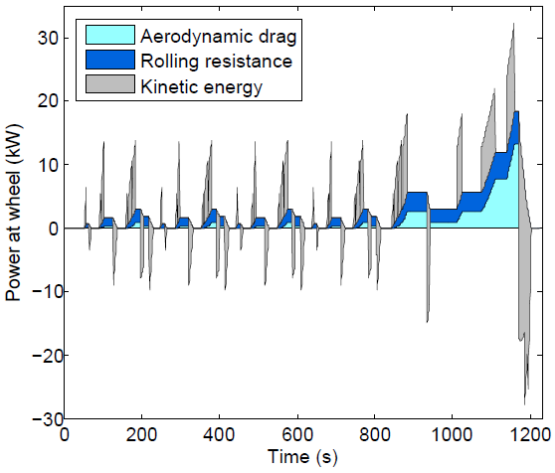

Figure 3: Power at the wheel of the baseline vehicle on the NEDC.

In the case of conventional vehicles without recuperation, the energy consumption E_{conv} can be calculated by integrating the power demand at the wheel in traction phases, devided by the cycle average vehicle efficiency η_{veh}

$$E_{conv} = \frac{1}{\eta_{veh}} \cdot \int_{t \in trac} (P_a + P_r + P_m)\, dt \quad (5)$$

as described in [18]. Traction and braking phases are characterized by positive and negative P_w, respectively. Electric vehicles offer the possibility to recuperate parts of the kinetic energy used for acceleration by reconverting negative power at the wheel through the powertrain into electric energy in the battery. If η_{pt} and η_{rec} are the cycle average battery-to-wheel (BtW) and wheel-to-battery (WtB) efficiency, respectively, the energy consumption for an electric vehicle E_{ev} is given by

$$E_{ev} = \frac{1}{\eta_{pt}} \cdot \int_{t \in trac} (P_a + P_r + P_m)\, dt + \eta_{rec} \cdot \int_{t \in brake} (P_a + P_r + P_m)\, dt \quad (6)$$

Note that the sum in the second integral is negative, i.e. reduces the net energy consumption. η_{pt} and η_{rec} include the efficiencies of the components transmission, motor/inverter, and battery, in traction and braking phases

$$\eta_{pt} = \eta_{trans_{tr}} \cdot \eta_{mot/inv_{tr}} \cdot \eta_{bat_{dis}} \quad (7)$$

$$\eta_{rec} = \eta_{trans_{br}} \cdot \eta_{mot/inv_{br}} \cdot \eta_{bat_{ch}} \quad (8)$$

In general, the efficiency of energy conversion of the electric motor is different in motor and generator mode for the same speed and opposite torque demand/supply [18]. However, since no information on the efficiency of the motor considered was available in generator mode, we assume it to be the same as in motor mode. We also assume the same efficiency for battery charging and discharging [32, 28, 33]. With these assumptions the recuperation efficiency η_{rec} is equivalent to the battery-to-wheel efficiency η_{pt}.

As outlined in [18] the phases of traction, coasting, and braking can be separated by calculating the coasting velocity. Based on this approach the contributions of P_a, P_r, and P_m to the mechanical energy demand and hence energy consumption can be evaluated as a function of vehicle and driving cycle dependent coefficients

$$E_{ev} = \frac{1}{\eta_{pt}} \cdot (A\, c_d\, A_f + B\, c_r\, m + C\, m) + \eta_{rec} \cdot (A'\, c_d\, A_f + B'\, c_r\, m + C'\, m) \quad (9)$$

where m is the vehicle mass including the rotational inertia of the wheels and motor rotor, and A, B, C, A′, B′, and C′ are driving cycle parameters. Table 2 lists the coefficients calculated for NEDC, the urban FTP-75, the highway HWFET, and the Artemis 130 driving cycles.

Table 2: Mechanical energy demand parametrization coefficients for the NEDC, the FTP-75, the HWFET, and the Artemis 130 driving cycles.

	NEDC	FTP-75	HWFET	Artemis 130
A	19100	12600	29200	36200
B	840	730	900	780
C	11.2	15.9	4.4	14.0
A'	2890	2870	2100	5450
B'	140	250	90	200
C'	-11.2	-15.9	-4.4	-14.0

Figure 4 shows the contributions of the aerodynamic drag, rolling resistance, and kinetic energy to the mechanical energy demand at the wheel of the baseline vehicle specified in Table 1 on the four considered cycles. Obviously the aerodynamic drag is more important in the highway cycle HWFET part due to higher speeds whereas the kinetic energy fraction is higher in the urban FTP-75 cycle due to more acceleration phases. The recuperable part of the total energy demand is higher in urban than highway driving due to a higher fraction of kinetic to total energy and a higher relative fraction of recuperable kinetic energy.

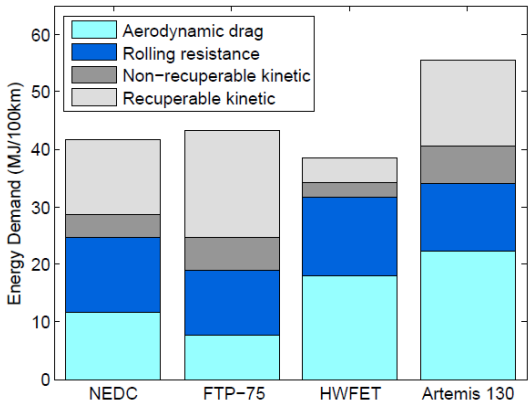

Figure 4: Mechanical energy demand of the baseline BEV on the NEDC, FTP-75, HWFET, and Artemis 130.

The battery-to-wheel energy consumption $\mathrm{E_{btw}}$ is calculated by taking into consideration the energy demand of accessory loads $\mathrm{P_{acc}}$

$$\mathrm{E_{btw}} = \mathrm{E_{ev}} + \frac{\int \mathrm{P_{acc}}\,\mathrm{dt}}{\eta_{\mathrm{bat}}} \tag{10}$$

For the calculation of the electricity cost to the consumer additional energy losses of the battery charger are taken into account. At modest charging levels (3 kW) an AC/DC battery charger operates with an efficiency η_{ch} of about 92% [32, 33, 35]. With this the plug-to-wheel energy consumption $\mathrm{E_{ptw}}$ is

$$\mathrm{E_{ptw}} = \frac{\mathrm{E_{btw}}}{\eta_{\mathrm{ch}}} \tag{11}$$

Based on Eq.(9-11) the sensitivity of energy consumption to mass (keeping other vehicle characteristics unchanged) can be assessed by calculating the partial derivatives

$$\frac{\partial \mathrm{E_{btw}}}{\partial \mathrm{m}} = \frac{1}{\eta_{\mathrm{pt}}} \cdot (\mathrm{B}\,\mathrm{c_r} + \mathrm{C}) + \eta_{\mathrm{rec}} \cdot (\mathrm{B'}\,\mathrm{c_r} + \mathrm{C'}) \tag{12}$$

$$\frac{\partial \mathrm{E_{ptw}}}{\partial \mathrm{m}} = \frac{\partial \mathrm{E_{btw}}}{\partial \mathrm{m}} / \eta_{\mathrm{ch}} \tag{13}$$

The calculated BtW and PtW energy consumption for the baseline vehicle on the NEDC, as well as the partial derivatives with respect to mass, are summarized in Table 3. Note that the energy consumption can be significantly higher at extreme weather conditions and/or aggressive driving.

2.3 Baseline vehicle cost structure today and in 2030

In this section we estimate the manufacturing costs of BEVs in 2012, 2020, and 2030 for the baseline configuration, i.e. without the application of lightweight materials. This is done by assessing the costs of components that are common with conventional vehicles, plus the costs for additional key components needed in a BEV, similar to the approach followed in [36, 37, 7, 38, 39, 34].

Table 3: Simulation results of energy consumption and mass sensitivity for the baseline BEV on the NEDC.

$\mathrm{E_{btw}}$ $(\frac{\mathrm{kWh}}{100\mathrm{km}})$	15.4
$\mathrm{E_{ptw}}$ $(\frac{\mathrm{kWh}}{100\mathrm{km}})$	16.7
$\frac{\partial \mathrm{E_{btw}}}{\partial \mathrm{m}}$ $(\frac{\mathrm{Wh}}{\mathrm{kg}\cdot 100\mathrm{km}})$	5.2
$\frac{\partial \mathrm{E_{ptw}}}{\partial \mathrm{m}}$ $(\frac{\mathrm{Wh}}{\mathrm{kg}\cdot 100\mathrm{km}})$	5.7

Total manufacturing costs of the glider components, i.e. body-in-white, closures, chassis, suspension, single gear transmission, interior, and low-voltage electrical equippment are taken for a medium size conventional vehicle from [1, 36, 25]. No future cost reductions are assumed for these mature components. Additional components considered for the BEV are a Li-ion battery pack, permanent magnet motor, inverter, controller, high voltage wiring, a DC/DC converter for supply of accessory loads, and a 3kW charger. The largest fraction of the battery costs increases linearly with battery capacity (for the considered battery capacity of the baseline BEV approximately 97%), and similarly costs of the motor and inverter scale linearly with motor power output. In this sense, additional BEV components are divided into variable costs which scale linearly with capacity and power, and fixed costs that are independent of battery energy content and motor power. Fixed components include high-voltage wiring, DC/DC converter, charger, and some battery and motor safety and control parts.

Due to technology improvements and the effects of increased production volume of electric vehicles, the weight and cost of BEV components is expected to decrease in the future. This effect is anticipated to be particularly pronounced for Li-ion batteries due to new electrode and electrolyte materials of next-generation batteries [43, 44, 45], and strong expected growth of global electric vehicle production [46]. Figure 5 shows projections for Li-ion battery pack costs from some recent studies [22, 40, 41, 42]. All assume cost reductions due to a combination of technical advances and mass production effects based on rising sales volume of electric vehicles and Li-ion batteries. If a range of values was indicated it is shown here as an arithmetic mean.

Battery and motor component costs used in this section are based on [22]. Table 4 summarizes the assumed specific mass $\mathrm{SM_b}$, $\mathrm{SM_p}$, and specific cost $\mathrm{SC_b}$, $\mathrm{SC_p}$ of variable battery and motor components, i.e. parts of the battery and motor/inverter that scale linearly with battery energy content and motor power, respectively. Note that

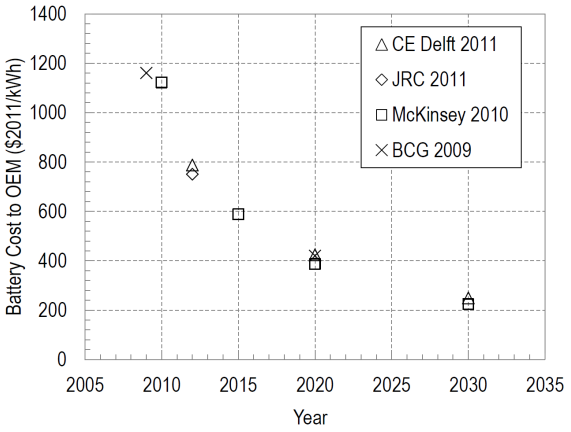

Figure 5: Projections of Li-ion battery costs [22, 40, 41, 42].

these costs are expected to be the high volume, unsubsidised costs to the vehicle manufacturer.

Table 4: Assumed specific mass and cost for battery and motor/inverter components [22].

	2012	2020	2030
SM_b ($\frac{kg}{kWh}$)	9.5	6.9	4.2
SM_p ($\frac{kg}{kW}$)	0.91	0.81	0.70
SC_b ($\frac{\$}{kWh}$)	775	413	238
SC_p ($\frac{\$}{kW}$)	22.5	18.0	14.4

Due to the expected improvements in battery energy and motor power density, the specific mass of both components decreases. This analysis aims to compare future BEVs having the same performance and range as assumed for the baseline vehicle described for 2012 in Table 1. Due to the reduction in specific mass, the future BEV with same range and performance will be lighter and as a consequence will consume less energy. The weight reduction at constant range R and performance due to reduction of specific masses of battery and motor in the future can be estimated as described in Eq.(14-16). Range is defined here as the maximum range that can be reached at full battery discharge, and performance as the initial power to mass ratio $\frac{P_0}{m_0}$, which is approximately inverse proportional to the acceleration time. In Eq.(14) the total new mass m of the vehicle is expressed as the sum of the new battery m_b, motor m_p, and glider mass m_{gl} (including the mass of fixed battery and powertrain parts). In Eq.(16), the new energy consumption E_{btw} is expressed as the original consumption E_{btw_0} minus the reduction due to weight reduction. Note that in this analysis no additional future energy consumption reductions due to, e.g., powertrain efficiency improvements are assumed.

$$m = m_b + m_p + m_{gl} \tag{14}$$

$$= R \cdot E_{btw} \cdot SM_b + \frac{P_0}{m_0} \cdot m \cdot SM_p + m_{gl} \tag{15}$$

$$= R \cdot \left(E_{btw_0} - \frac{\partial E_{btw}}{\partial m} \cdot (m_0 - m)\right) \cdot SM_b + \frac{P_0}{m_0} \cdot m \cdot SM_p + m_{gl} \tag{16}$$

Solving for the new vehicle mass yields

$$m = \frac{R \cdot SM_b \cdot (E_{btw_0} - \frac{\partial E_{btw}}{\partial m} \cdot m_0) + m_{gl}}{1 - \frac{P_0}{m_0} \cdot SM_p - \frac{\partial E_{btw}}{\partial m} \cdot R \cdot SM_b} \tag{17}$$

Based on Eq.(17), the mass and energy consumption of the baseline BEV configuration in the year 2020 and 2030 are adjusted relative to the BEV in 2012 to account for the lower specific mass of battery and motor/inverter in 2020 and 2030 according to Table 4. The baseline BEV characteristics, and the cost and weight structure for 2012, 2020, and 2030 are summarized in Table 5. Note that range, performance, and the values of A_f, c_d, and c_d are held constant. The ratio of 1.3 of the purchase price of the BEV in 2012 (Table 1) and total manufacturing costs as given in Table 5 is in good agreement with a review of retail price equivalent markup factors in [1].

2.4 Powertrain resizing

In the following the resizing effects of a smaller required battery and motor when lightweighting the glider at constant range and peformance are examined. Glider lightweighting reduces the BtW energy consumption as described in section 2.2. The reduced energy consumption results in a lighter powertrain due to a smaller necessary battery and motor at constant range and performance. This first order effect in turn reduces energy consumption further and higher order secondary mass reductions are achieved. This recursive sequence is described by Eq.(18,19), where Δm_{gl} is the glider mass reduction due to the application of lightweight materials

$$m[0] = m_0 \tag{18}$$

$$m[n+1] = m_0 - \Delta m_{gl} - m_b \cdot \left(1 - \frac{E_{btw}}{E_{btw_0}}\right) - m_p \cdot \left(1 - \frac{m[n]}{m_0}\right) \tag{19}$$

which converges to

$$m = m_0 - \frac{m_b + \Delta m_{gl} - \frac{E_{btw}}{E_{btw_0}} \cdot m_b}{1 - \frac{m_p}{m_0}} \tag{20}$$

Table 5: Baseline BEV characteristics, weight and cost structure in 2012, 2020, and 2030 keeping range and performance constant.

	2012		2020		2030	
$EC_{btwNEDC}$ ($\frac{kWh}{100km}$)	15.4		15.0		14.6	
Battery capacity (kWh)	25		24.3		23.6	
Range (km)	162		162		162	
Power (kW)	87		82		87.5	
Power/mass ($\frac{W}{kg}$)	58		58		58	
	Mass (kg)	Cost ($)	Mass (kg)	Cost ($)	Mass (kg)	Cost ($)
Glider (+ stable parts)	1183	11500	1183	11500	1183	11500
Variable parts						
Battery	238	19375	168	10023	98.4	5610
Motor, Inverter	87	1958	82	1479	77.5	1114
Total manufacturing	1500	32832	1417	23002	1336	18222

From this the total vehicle mass reduction relative to primary glider mass reduction $\frac{\Delta m}{\Delta m_{gl}}$ follows

$$\begin{aligned}\frac{\Delta m}{\Delta m_{gl}} &= \frac{m - m_0}{\Delta m_{gl}} \\ &= \frac{m_b + \Delta m_{gl} - \frac{E_{btw}}{E_{btw_0}} \cdot m_b}{m_{gl} \cdot (1 - \frac{m_p}{m_0})} \end{aligned} \quad (21)$$

Eq.(20,21) depend on the new energy consumption E_{btw} of the lightweighted vehicle which is a priori not known. E_{btw} can be either calculated iteratively for each level of lightweighting applied, or by solving a second recursive equation which results in a solution for $\frac{\Delta m}{\Delta m_{gl}}$ as a function of m_{gl} applied. To do so, the new energy consumption is expressed as a function of Δm_{gl} and $\frac{\partial E_{btw}}{\partial m}$

$$\begin{aligned}E_{btw} &= E_{btw_0} - \frac{\partial E_{btw}}{\partial m_{gl}} \cdot \Delta m_{gl} \\ &= E_{btw_0} - \frac{\partial E_{btw}}{\partial m} \cdot \frac{\Delta m}{\Delta m_{gl}} \cdot \Delta m_{gl} \end{aligned} \quad (22)$$

Substituting Eq.(21) in (22) we find the recursive function for E_{btw}

$$E_{btw}[0] = E_{btw_0} \quad (23)$$

$$\begin{aligned}E_{btw}[n+1] = E_{btw_0} &- \frac{\partial E_{btw}}{\partial m} \\ &\cdot \frac{(m_b + \Delta m_{gl} - \frac{E_{btw}[n]}{E_{btw_0}} \cdot m_b)}{(1 - \frac{m_p}{m_0})} \end{aligned} \quad (24)$$

which converges to

$$\begin{aligned}E_{btw} = E_{btw_0} &\\ &- \frac{\frac{\partial E_{btw}}{\partial m} \cdot m_0 \cdot \Delta m_{gl}}{(m_0 - m_p) - \frac{\partial E_{btw}}{\partial m} \cdot \frac{m_0 \cdot m_b}{E_{btw_0}}} \end{aligned} \quad (25)$$

Substituting Eq.(25) in (21) yields

$$\frac{\Delta m}{\Delta m_{gl}} = \frac{1}{1 - \frac{m_p}{m_0} - \frac{\partial E_{btw}}{\partial m} \cdot \frac{m_b}{E_{btw_0}}} \quad (26)$$

This factor indicates the change of total vehicle mass to primary glider weight reduction. It includes the achieved powertrain mass reduction $\Delta m_{pt} = \Delta m_b + \Delta m_m$ of battery and motor that can be achieved at constant range and power to mass ratio. It is a function of the initial vehicle, battery and motor mass, initial energy consumption, and the partial derivative of energy consumption with respect to mass (which was determined in section 2.2). Accordingly the total powertrain mass reduction due to resizing the battery and motor (keeping range and performance constant) relative to the applied glider mass reduction is

$$\begin{aligned}\frac{\Delta m_{pt}}{\Delta m_{gl}} &= \frac{\Delta m - \Delta m_{gl}}{\Delta m_{gl}} \\ &= \frac{1}{1 - \frac{m_p}{m_0} - \frac{\partial E_{btw}}{\partial m} \cdot \frac{m_b}{E_{btw_0}}} - 1 \end{aligned} \quad (27)$$

In the preceeding equations the initial battery mass can be equally expressed as a function of the range R and the specific battery mass SM_b: $m_b = R \cdot E_{btw_0} \cdot SM_b$, and the initial motor mass as $m_p = P \cdot SM_p$. Substituting in Eq.(27) yields

$$\frac{\Delta m_{pt}}{\Delta m_{gl}} = \frac{1}{(1 - \frac{\partial E_{btw}}{\partial m} \cdot R \cdot SM_b - \frac{P}{m} \cdot SM_p)} - 1 \quad (28)$$

which is a simple, analytical expression for the estimation of battery and motor mass reduction that can be achieved with lightweighting the glider at a given range and performance. Note that battery and motor sizing effects investigated in this section also define achievable powertrain cost reductions as cost an mass are linearly related. The cost implications are outlined in the next section.

2.5 Cost minimization and scenario analysis

2.5.1 Baseline scenario

As described in section 2.3 total manufacturing costs for the baseline BEV configration are the sum of glider, battery, and motor costs. With the application of lightweighting, additional costs according to Eq.(3) have to be taken into account. In order to find the optimal implementation of lightweighting, total manufacturing costs C_{man} are decomposed into baseline costs C_{bl}, lightweighting costs C_{lw}, and cost reductions due to a smaller required battery CR_b and motor CR_p

$$C_{man} = C_{bl} + C_{lw} - CR_b - CR_p \quad (29)$$

CR_b and CR_p are based on the assumption of constant range R and performance $\frac{P}{m}$ and are expressed as a function of lightweighting applied

$$CR_b = CRF_b \cdot SC_b \cdot \left(R \cdot (EC_{btw_0} - EC_{btw})\right) \quad (30)$$

$$CR_p = CRF_p \cdot SC_p \cdot \left(P_0 - \frac{P}{m} \cdot (m_0 - \Delta m)\right) \quad (31)$$

where EC_{btw} and Δm are expressed according to Eq.(25, 26) with Δm_{gl} replaced by Δm_{lw}. The cost minimum is found by setting the partial derivative $\frac{\partial C_{man}}{\partial \Delta m_{lw}}$ to zero

$$\frac{\partial C_{man}}{\partial \Delta m_{lw}} = 0 \quad (32)$$

The solution for optimal weight reduction $\Delta m_{lw_{opt}}$ is parameterized as a function of specific battery and powertrain costs, lightweighting marginal costs, and associated cost reduction factors. A tipping point for marginal lightweighting cost $MC_{lw_{tip}}$ exists up to which the application of lightweighting reduces manufacturing costs. Total costs, C_{tot} are calculated as manufacturing costs plus vehicle lifetime electricity costs for 120'000 km of travel, PtW energy consumption as defined in Eq.(11), and average US retail price of electricity to ultimate customers in residential sector according to [50]. The optimal weight reduction minimizing total costs is equally found analytically by setting the partial derivative to zero and solving for $\Delta m_{lw_{opt}}$. Future electricity savings are not discounted. To solely analyze the impacts of the trend towards declining technology and rising electricity costs, no difference in battery, motor, and lightweighting cost reduction is assumed, i.e. the sames cost reduction factors are applied in this scenario: CRF = 0.6 in 2020, and 0.4 in 2030.

Table 6: Assumed electricity price according to [50].

	2012	2020	2030
SC_{el} ($\frac{\$cent}{kWh}$)	11.7	12.9	15.4

The breakdown of manufacturing and electricity cost as a function of applied glider mass reduction through lightweighting, is shown in Figure 6. The optimization results in this scenario are summarized in Table 7. Optimal glider mass reduction is found to be 450 and 490 kg in 2012, reducing manufacturing costs by 4.9% and total costs by 4.6%, respectively. As a result of the assumed reduction of battery and motor costs, higher cost savings with lightweighting can be achieved today than in future. The reduction of BEV component costs and the increase of electricity price leads to a higher relative share of electricity to total costs in the future, which in turn increases the gap between the optimal solutions based on minimizing manfacturing versus total costs. Whether the optimum level of weight reduction will decrease or increase depends on the relative development of battery vs. lightweighting costs.

Table 7: Optimization results in the baseline scenario.

	2012	2020	2030
Manufacturing costs			
$\Delta m_{lw_{opt}}$(kg)	450	437	423
ΔC_{man}(%)	4.9	3.7	2.8
$MC_{lw_{tip}}$($\frac{\$}{kg}$)	9.1	5.3	3.4
Manufacturing and electricity costs			
$\Delta m_{lw_{opt}}$(kg)	490	506	540
ΔC_{tot}(%)	4.6	3.3	2.2
$MC_{lw_{tip}}$($\frac{\$}{kg}$)	10.0	6.2	4.5

2.5.2 Sensitivity analysis

The analytic form of the solution allows one to analyse the dependence of the optimization results with respect to all input parameters as

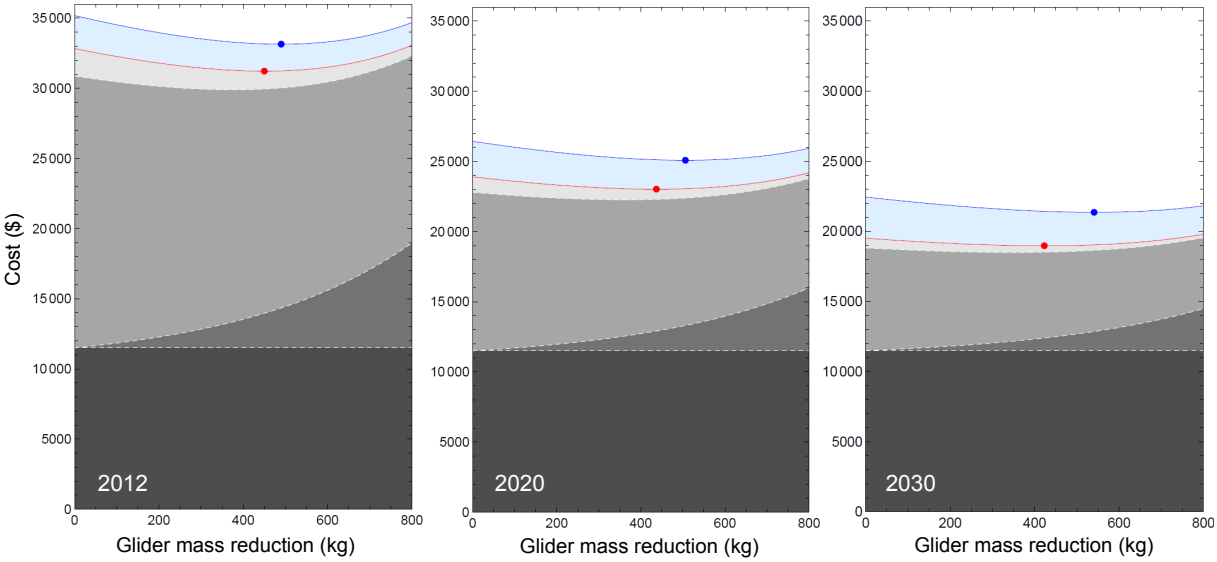

Figure 6: Breakdown of OEM manufacturing and electricity cost as a function of primary mass reduction for the baseline scenario in 2012, 2020, 2030. Red points indicate minimal manufacturing costs, blue points minimal total costs.

well as to adjust the solution to a certain scenario. This section investigates the sensitivity of optimal mass reduction with respect to the assumed cost reduction factors for principal components. As shown in Figure 6, battery and at a higher degree of mass reduction also lightweighting costs are the two main contributors to manufacturing costs. Figure 7 shows the sensitivity of optimal mass reduction minimizing manufacturing costs to lightweighting and battery costs for 2012, 2020, and 2030. Each surface indicates the sensitivity of optimal mass reduction within a range of 20% higher to 20% lower lightweighting and battery cost reduction as assumed for this scenario which is represented by a red point for the respective year. The analysis shows that the sensitivity of optimal weight reduction increases in the future as a result of the less well defined cost minimum.

Figure 8 shows the optimal weight reduction minimizing total costs as a function of the electricity price. Note that if for example the electricity is generated in solar PV plants for which levelized cost are approximately a factor of 2.2 higher [50], optimal mass reduction is considerably higher than for the electricity prices used in this scenario. At zero electricity cost the solution is equal to optimal mass reduction minimizing manufacturing cost.

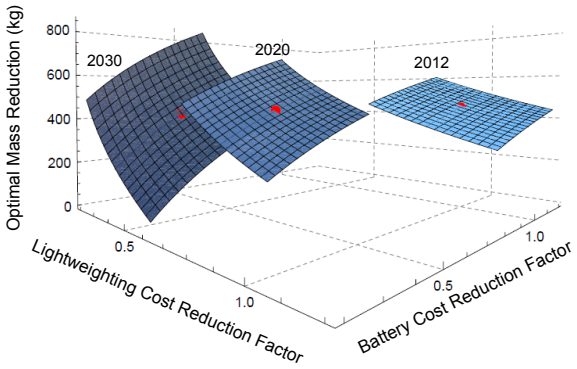

Figure 7: Optimal weight reduction minimizing manufacturing costs. Red points indicate the baseline values and each surface the sensitivity of optimal mass reduction within a range of 20% higher to 20% lower lightweighting and battery cost reduction factors.

3 Conclusion

This paper presents a concise, analytic methodology to determine the optimal amount of lightweighting for BEVs. This is based on minimizing the marginal costs of vehicle lightweighting with the cost reductions due to a smaller battery and motor required to maintain constant

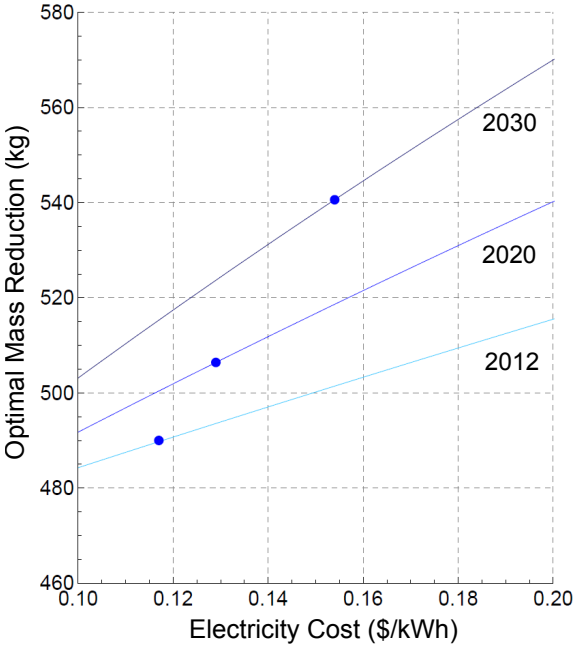

Figure 8: Optimal weight reduction minimizing total manufacturing and electricity costs as a function of electricity price. Blue points indicate the baseline value for the respective year.

range and performance. The powertrain resizing effect is analytically determined. Current technology costs indicate that for the baseline BEV, optimal glider mass reduction of about 450 kg leads to manufacturing cost reductions of 4.9%. It is shown that declining battery and motor costs reduce the absolute importance of lightweighting in reducing BEV costs over time, and that rising electricity costs increase the gap between the optimal solutions, based on minimizing manufacturing vs. total costs. Whether the optimum level of weight reduction will decrease or increase depends on the relative development of battery vs. lightweighting costs. The sensitivity of the optimal lightweighting to critical cost parameters has been evaluated, and is shown to increase over time.
In addition to cost and range, other criteria such as safety and environmental impacts are also important to consumers and the society. Vehicle manufacturers should consider these aspects in their decision about the best lightweighting strategy. The methodology presented in this paper allows the potential economic benefits of lightweighting to be determined early in the vehicle development process. It can be easily modified to be applied to other drivetrain types and vehicle market segments, and to include other optimization objectives.

Acknowledgments

This research was carried out within the project Technology-centered Electric Mobility Assessment (THELMA), sponsored by the Swiss Competence Center for Energy & Mobility, Swiss Electric Research, and the Erdoel-Vereinigung.

References

[1] National Research Council, *Assessment of Fuel Economy Technologies for Light-Duty Vehicles*, The National Academies Press, Washington D.C., 2011.

[2] J. DeCicco et al., *Technical Options for Improving the Fuel Economy of US Cars and Light Trucks by 20102015*, American Council for an Energy Efficient Economy, Washington, D.C., 2001.

[3] EPA Staff Technical Report, *Cost and Effectiveness Estimates of Technologies Used to Reduce Light-duty Vehicle Carbon Dioxide Emissions*, EPA420-R-08-008, United States Environment Protection Agency, 2008.

[4] H. Kim et al., *Economic Assessment of Greenhouse Gas Emissions Reduction by Vehicle Lightweighting Using Aluminum and High-Strength Steel*, Journal of Industrial Ecology 15, 1, 64 - 80, 2010.

[5] I. Skinner et al., *Assessment with respect to long term CO2 emission targets for passenger cars and vans*, Deliverable D2: Final Report, ED45757, 2009.

[6] E. Wilhelm et al., *Optimal Implementation of Lightweighting and Powertrain Efficiency Technology in Passenger Vehicles*, Accepted in Transport.

[7] M.A. Delucchi et al. *Electric and Hybrid Vehicles, Chapter Two - Lifetime Cost of Battery, Fuel-Cell, and Plug-in Hybrid Electric Vehicles*, Elsevier, 19-60, 2010.

[8] A. Joshi et al., *Optimizing Battery Sizing and Vehicle Lightweighting for an Extended Range Electric Vehicle*, SAE Technical Paper 2011-01-1078, 2011.

[9] L. Cheah et al., *Factor of Two: Halving the Fuel Consumption of New U.S. Automobiles by 2035*. Massachusetts Institute of Technology, Publication No. LFEE 2007-04 RP, 2007.

[10] L. Cheah, *Cars on a Diet: The Material and Energy Impacts of Passenger Vehicle Weight Reduction in the U.S.*, PhD Thesis, Engineering Systems Division, Massachusetts Institute of Technology, 2010.

[11] N. Lutsey, *Review of Technical Literature and Trends Related to Automobile Mass-Reduction Technology*, University of California, Davis, Prepared for California Air Resources Board, 2010.

[12] Lotus Engineering Inc., *An Assessment of Mass Reduction Opportunities for a 2017-2020 Model Year Vehicle Program*, 2010.

[13] World Auto Steel, *Future Steel Vehicle*, 2011.

[14] IBIS Associates Inc., *Aluminum Vehicle Structure: Manufacturing and Lifecycle Cost Analysis Hybrid Drive and Diesel Vehicles*, Report 2008-05, Prepared for the Aluminum Association, 2008.

[15] M. Goede et al., *Super Light Car lightweight construction thanks to a multi-material design and function integration*, European Transport Research Review 1, 5-10, 2009.

[16] A.B. Lovins et al., *Hypercars, hydrogen, and the automotive transition*, Int. J. Vehicle Design 35, 50-85, 2004.

[17] M. Gruenig et al., *Impacts of Electric Vehicles - Deliverable 1 An overview of Electric Vehicles on the market and in development*, Delft, CE Delft, 2011.

[18] L. Guzzella, A. Sciarretta, *Vehicle propulsion systems modeling and optimization*, Berlin, Springer Verlag, 2007.

[19] R. Joumard et al., *Influence of driving cycles on unit emissions from passenger cars*, Atmospheric Environment 34, 4621-4628, 2000.

[20] C. Silva et al., *Analysis and simulation of low-cost strategies to reduce fuel consumption and emissions in conventional gasoline light-duty vehicles*, Energy Conversion and Management, 50, 215-222, 2009.

[21] D.W. Gao et al., *Modeling and Simulation of Electric and Hybrid Vehicles*, Proceedings of IEEE, 95, 729-745, 2007.

[22] G. Duleep et al., *Impacts of Electric Vehicles - Deliverable 2 Assessment of electric vehicle and battery technology*, Delft, CE Delft, 2011.

[23] A. Emadi et al., *Power Electronics and Motor Drives in Electric, Hybrid Electric, and Plug-In Hybrid Electric Vehicles*, IEEE Transactions on Industrial Electronics, 55, 2237-2245, 2008.

[24] S.S. Williamson et al., *Comprehensive Efficiency Modeling of Electric Traction Motor Drives for Hybrid Electric Vehicle Propulsion Applications*, IEEE Transaction on Vehicular Technology, 56, 1561-1571, 2007.

[25] M.A. Kromer et al., *Electric Powertrains: Opportunities and. Challenges in the U.S. Light-Duty Vehicle Fleet*, LFEE 2007-03, 2007.

[26] R. Farrington et al., *Impact of Vehicle Air-Conditioning on Fuel Economy, Tailpipe Emissions, and Electric Vehicle Range*, NREL/CP-540-28960, 2000.

[27] S.A. Rogers et al., *Evaluation of 2004 Toyota Prius Hybrid Electric Drive System*, ORNL/TM-2006/423, 2006.

[28] S. Campanari et al., *Energy analysis of electric vehicles using batteries or fuel cells through well-to-wheel driving cycle simulations*, Journal of Power Sources, 186, 464 - 477, 2009.

[29] R. Ravishankar et al., *Battery Modeling for Energy-Aware System Design*, Computer, 36, 77-87, 2003.

[30] T.K. Dong et al., *Dynamic Modeling of Li-Ion Batteries Using an Equivalent Electrical Circuit*, Journal of the Electrochemistry Society, 158, 326-336, 2011.

[31] M. Doyle et al., *Modeling of Galvanostatic Charge and Discharge of the Lithium/Polymer/Insertion Cell*, Journal of the Electrochemical Society, 140, 1526-1533, 1993.

[32] D.A. Howey et al., *Comparative measurements of the energy consumption of 51 electric, hybrid and internal combustion engine vehicles*, Transportation Research Part D 16, 459-464, 2011.

[33] M. Zackrisson et al., *Life cycle assessment of lithium-ion batteries for plug-in hybrid electric vehicles*, Journal of Cleaner Production, 18, 1519-1529, 2010.

[34] C. Thiel et al., *Cost and CO2 aspects of future vehicle options in Europe under new energy policy scenarios*, Energy Policy, 38, 7142-7151, 2010.

[35] S. Eaves, *A cost comparison of fuel-cell and battery electric vehicles*, Journal of Power Sources, 130, 208-212, 2004.

[36] R.M. Cuenca et al., *Evaluation of Electric Vehicle Production and Operating Costs*, ANL/ESD-41, 1999.

[37] M.A. Delucchi et al. *An analysis of the retail and lifecycle cost of battery-powered electric vehicles*, Transportation Research Part D, 6, 371-404, 2001.

[38] G.J. Offer et al., *Comparative analysis of battery electric, hydrogen fuel cell and hybrid vehicles in a future sustainable road transport system*, Energy Policy, 38, 24-29, 2010.

[39] G.J. Offer et al., *Techno-economic and behavioural analysis of battery electric, hydrogen fuel cell and hybrid vehicles in a future sustainable road transport system in the UK*, Energy Policy, 39, 1939-1950, 2011.

[40] Concawe/JRC/EUCAR, *Well-to-Wheels Analysis of Future Automotive Fuels and Powertrains in the European Context*, Version 3c, 2011.

[41] Boston Consulting Group, *Batteries for Electric Cars: Challenges, Opportunities and the Outlook to 2020*, Report, 2009.

[42] McKinsey&Company, *A portfolio of powertrains for Europe: a fact-based analysis*, Report, 2010.

[43] P. Bruce et al., *LiO2 and LiS batteries with high energy storage*, Nature Materials, 11, 19-29, 2011.

[44] J. Xiulei et al., *A highly ordered nanostructured carbonsulphur cathode for lithiumsulphur batteries*, Nature Materials, 8, 500-506, 2009.

[45] A. Magasinski et al., *High-performance lithium-ion anodes using a hierarchical bottom-up approach*, Nature Materials, 9, 353-358, 2010.

[46] International Energy Agency, *Energy Technology Perspectives 2010*, OECD/IEA, 2010.

[47] E. Alonso et al., *Evaluating the Potential for Secondary Mass Savings in Vehicle Lightweighting*, Environ. Sci. Technol., 2012.

[48] C. Bjelkengren, *The Impact of Mass Decompounding on Assessing the Value of Vehicle Lightweighting*, Master Thesis, Massachusetts Institute of Technology, 2008.

[49] M. Verbrugge et al., *Mass Decompounding and Vehicle Lightweighting*, Materials Science Forum 618-619, 411-418, 2009.

[50] U.S. Department of Energy, *Annual Energy Outlook 2011*, Energy Information Administration, DOE/EIA-0383, 2010.

Authors

Johannes Hofer studied Physics at LMU Munich with specializations in Quantum Optics and Industrial Engineering. Since 2010 he is working towards his PhD from ETH Zurich in the Technology Assessment group at the Paul Scherrer Institute. His focus is on electric vehicle simulation and fleet modeling.

Erik Wilhelm is a post-doctoral fellow in the Field Intelligence Lab at MIT. He earned his PhD from the ETH Zurich on heuristic vehicle design techniques while working in the Technology Assessment group at PSI. His focus is on advanced powertrain simulation and optimization methods.

Warren Schenler received a BS degree in Engineering Physics and PhD in Energy Systems and Policy at MIT. He came to PSI in 2001, and is now in the Technology Assessment Group within the Laboratory for Energy Systems Analysis. He is responsible for the economic cost analysis of electric power systems, including generation technologies, systems interactions and multi-attribute, multi-scenario analysis.